Silicon Mach-Zehnder Interferometer

Athira404

1. Introduction

On-chip Mach Zehender Interferometers (MZI) have attracted various applications ranging from biomedical sensing, optical switching, quantum computing, spectroscopy, and metrology [1-4]. Similar to the conventional MZI, the phase difference between the two light beams can be adjusted by creating an optical path difference between the two arms of the interferometer and further controlling the output using thermo-optic, electro-optic or refractive-index changes, making them suitable for different applications.

Here, a Mach-Zhender interferometer of different free spectral ranges (FSR) are designed. The theoretically calculated group index will be experimentally verified using measurements from the fabricated MZI. The next section describes the theory of MZI mostly adapted from [5].

2. Theory

A concept schematic of an MZI is provided in the Figure below. The input (complex) electric field **Ei** is equally divided into two at the first Y branch into **Ei1** and **Ei2** each having half the intensity of the incident light. Therefore,

$$Ei1 = \frac{Ei}{\sqrt{(2)}} \tag{1}$$

$$Ei2 = \frac{Ei}{\sqrt{(2)}} \tag{2}$$

At the time of recombining at the second Y branch, **Eo1** and **Eo2** evolve differently due to the difference in the optical path length difference. Assuming zero absorption and scattering losses, the two electric fields at the time of recombining becomes,

$$Eo1 = \frac{Ei}{\sqrt{2}} e^{i(\omega t - \beta L1)} \tag{3}$$

$$Eo2 = \frac{Ei}{\sqrt{2}} e^{i(\omega t - \beta L2)} \tag{4}$$

where β is the propagation constant, $L1$ and $L2$ are the path lengths traversed in each arm of the MZI.

Upon recombination at the combining Y splitter, the output electric field,

$$Eo = \frac{Eo1 + Eo2}{\sqrt{2}} = \frac{Ei}{2}(e^{-i\beta L1} + e^{-i\beta L2}) \tag{5}$$

The output intensity,

$$Io = (\frac{Ei}{2}(e^{-i\beta L1} + e^{-i\beta L2}))^2 \tag{6}$$

$$Io = \frac{Ii}{4}(1 + Cos(\beta \Delta L)) \tag{7}$$

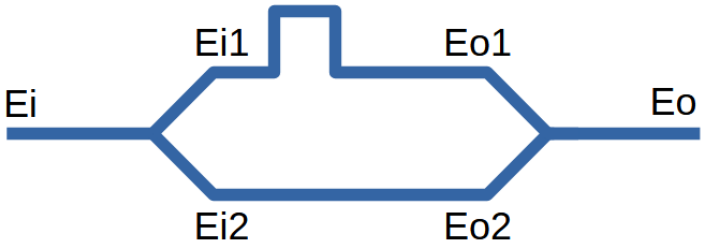

Fig. 1. Schematic of the MZI

The free spectral range (FSR) is the spectral difference between two consecutive peaks, which can be derived as

$$FSR = \frac{\lambda^2}{\Delta L * ng} \tag{8}$$

where ng is the group index. By measuring the FSR corresponding to different ΔL values, the group index can be calculated from the FSR values for each case ΔL.

3. Simulation and Design

Length diff. (um)	FSR Theoretical (nm)	FSR Numerical (nm)
30	17.8	18
60	9.53	9.68
90	6.36	6.32
120	4.77	4.77
150	3.81	3.79

The strip waveguide having 220 nm height and 500 nm width is chosen as the waveguide model. Figure 2 shows the quasi-TE mode of the waveguide at 1550 nm obtained using Lumerical MODE solver. The refractive index data corresponding to Si and SiO2 is chosen from Palik. The effective refractive index and the group index obtained after performing a wavelength sweep for the quasi-TE mode as a function of wavelengths are given in Figure 3 and Figure 4, respectively.

The Taylor series expansion of effective refractive index gives the expression:

$$neff(\lambda) = n1 + n2(\lambda - \lambda 0) + n3(\lambda - \lambda 0)^2 \tag{9}$$

Curve fitting of the effective refractive index versus wavelength in MATLAB gives the values of n1, n2 and n3 as 2.45, -1.13 and -0.04 respectively.

The group index value for the TE like mode at 1550 nm is estimated as 4.2. Based on this value, the following table summarizes the FSR values corresponding to different length deviations between the two arms of the MZI.

The following figures show the output gain as a function of wavelength for the different length differences of the interferometer arms.

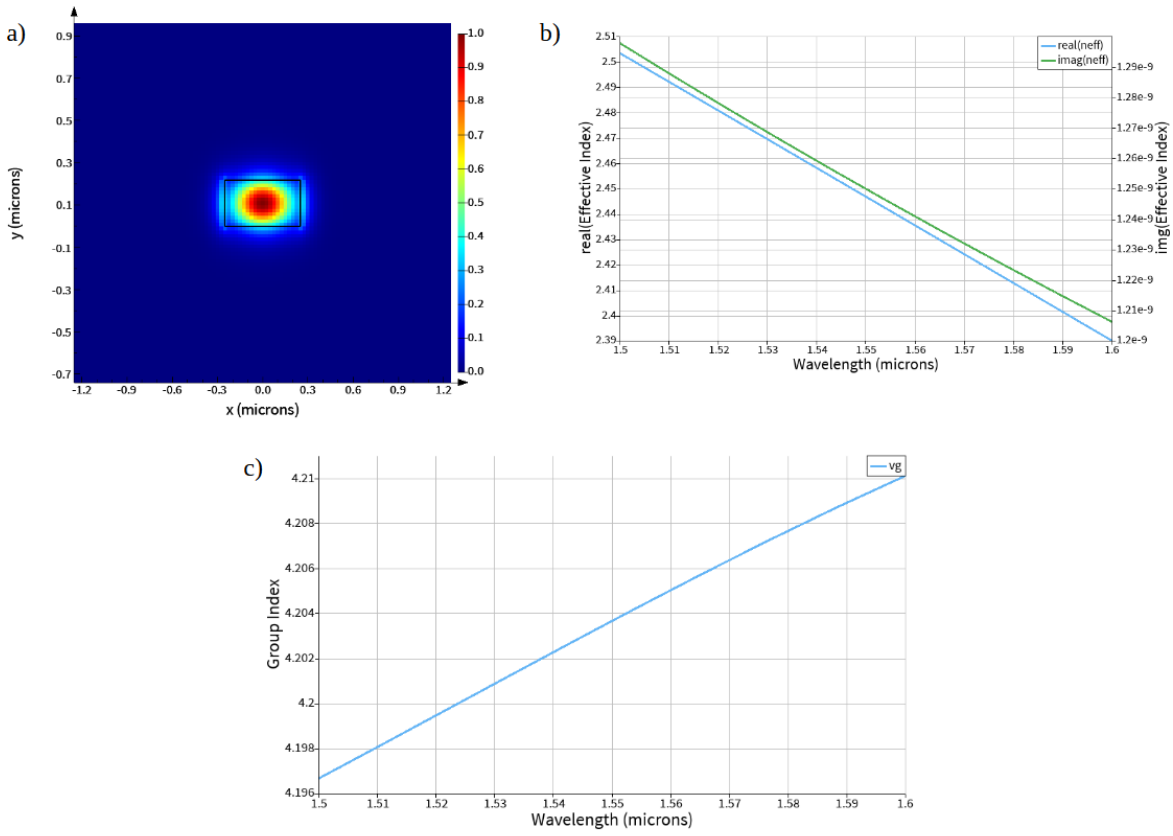

Fig. 2. a) The electric field intensity of the quasi-TE mode. b) The effective refractive index of the quasi-TE mode. c) The group index of the quasi-TE mode.

3.1. Corner Analysis

Fabrication imperfections can cause deviations in the waveguide mode, the effective refractive index, the group index, and thus the performance of the device. Here we assume the thickness of the Si Wafer to be 219.2 nm with a possible variation of 3.9 nm. Similarly, a minimum width of 470 nm and a maximum width of 510 nm are considered for the corner analysis. The variations in the effective index and group index corresponding to each scenario are listed in the table below. In the table below, + and - denote the positive and negative extremes of the parameters, respectively. The first sign corresponds to width, and the second one indicates the height.

Cases	neff	ng
ideal	2.5	4.2
++	2.46	4.26
+−	2.497	4.18
−+	2.45	4.26
−−	2.5	4.2

3.2. Layout

Figure 4 shows the file approved for fabrication, after the Design Rule Check (DRC) check.

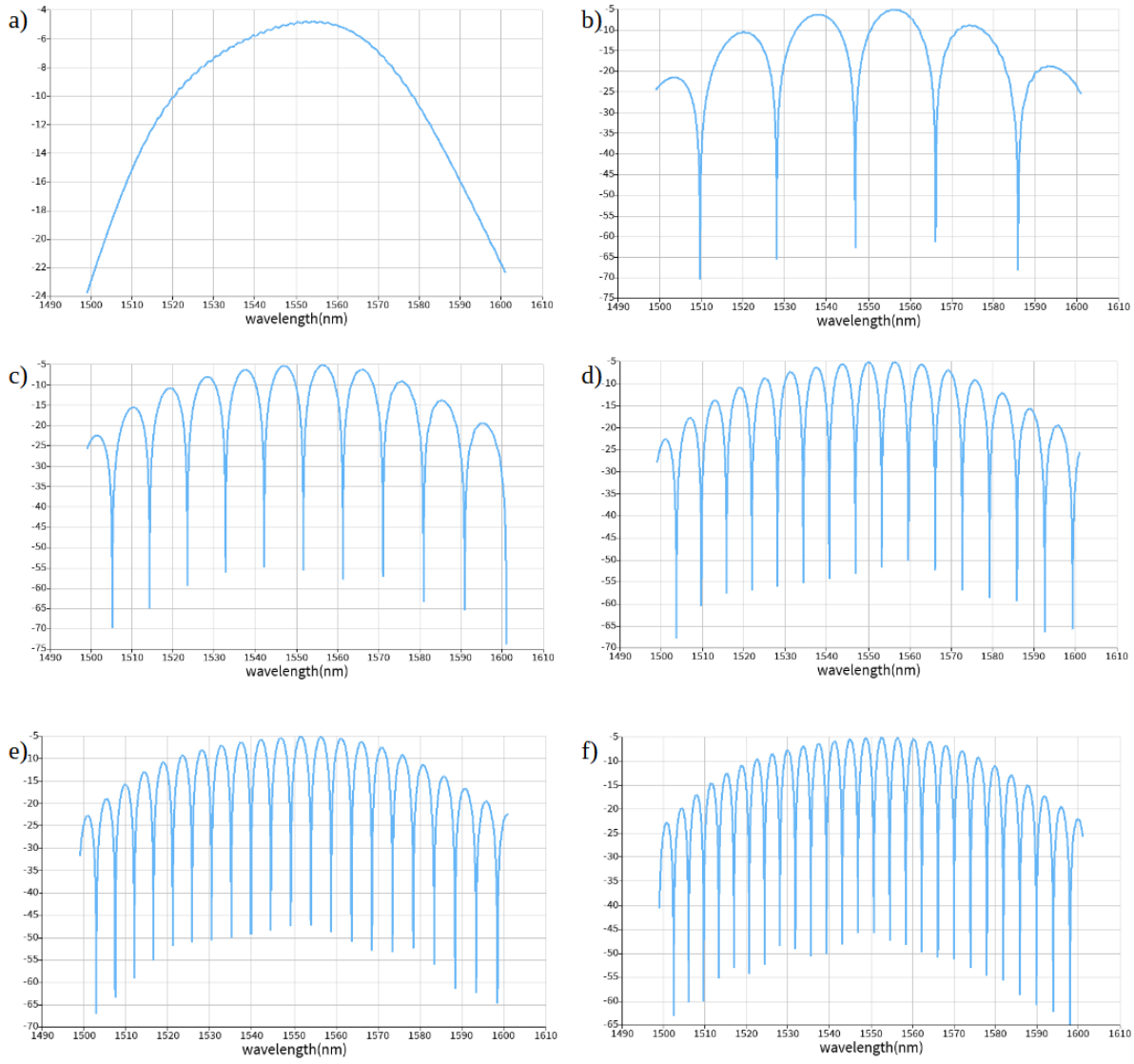

Fig. 3. Gain of the MZI as a function of wavelength a) grating coupler, b) ΔL=30, c) ΔL=60, d) ΔL=90, e) ΔL=120, f) ΔL=150.

3.3. Fabrication Method

Fabrication is performed using an electron beam lithography (EBL) facility at the Washington Nanofabrication Facility using the NanoSOI MPW fabrication process by Applied Nanotools Inc. (http://www.appliednt.com/nanosoi; Edmonton, Canada) [6]. Silicon-on-insulator wafers with 2 µm buffer oxide thickness are used as the base material for the fabrication. After cleaning, hydrogen silsesquioxane (HSQ) resist was spin-coated onto the substrate and heated to evaporate the solvent and then patterned using a JEOL JBX-8100FS electron beam instrument (at 100 keV energy, 8 nA beam current, and 500 µm exposure field size). After the e-beam exposure the development is done with a tetramethylammonium sulfate (TMAH) solution. Afterward, the ICP-RIE etch process using chlorine is performed. After removal of resist, a 2.2 µm oxide cladding was deposited using a plasma-enhanced chemical vapor deposition (PECVD) process at 300 ° C.

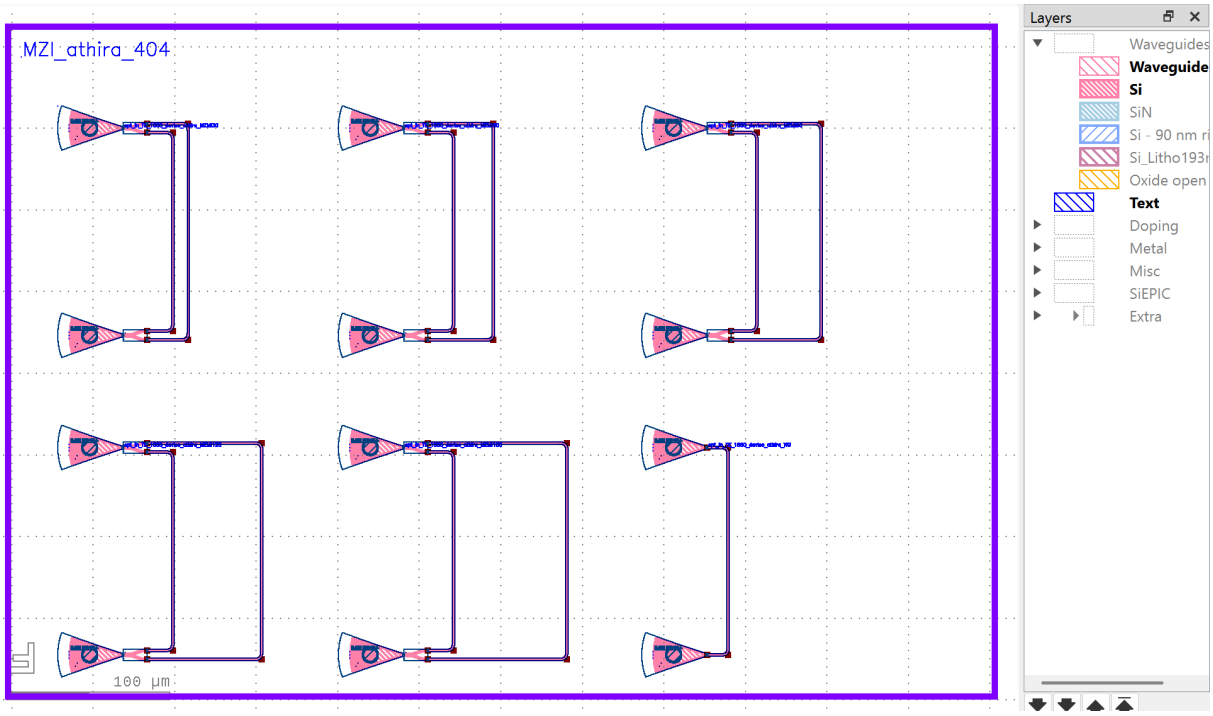

Fig. 4. Layout for the fabrication.

4. Experimental Results and Data Analysis

The devices are characterized using an automated test setup [7, 11]. A tunable laser was used as the input source and optical power sensors as the output detectors. The wavelength was swept from 1500 to 1600 nm in 10 pm steps. A polarization maintaining (PM) fibre was used to couple the light into the grating couplers [9]. The outputs of each MZI are plotted below, after subtracting the background obtained from a reference waveguide.

Based on the experimental measurements, the FSR values and group index values were calculated and summarized in the table below. The group refractive index can be calculated from the free spectral range of each experimental data. This value is plotted as a function of wavelength. The experimentally observed FSR (around 1550 nm) corresponding to the different path length deviations are listed in the table below. The calculated group indices for the TE mode (at 1550 nm) are 4.08, 4.16, 4.15, 4.17 and 4.16 corresponding to the path length differences of 30, 60, 90, 120 and 150 micrometers respectively. These values lie close to the range predicted by the corner analysis, indicating that the fabrication errors are within the expected range.

Length diff. (um)	FSR Exp. (nm)	ng
30	19.6	4.08
60	9.62	4.16
90	6.33	4.15
120	4.75	4.17
150	3.83	4.16

Approximating n1 to be 2.4, the initial parameters for n2 were determined as -1.08, -1.135, -1.129, -1.145, and -1.135 for each MZI in the increasing order of path difference from 30 μm to

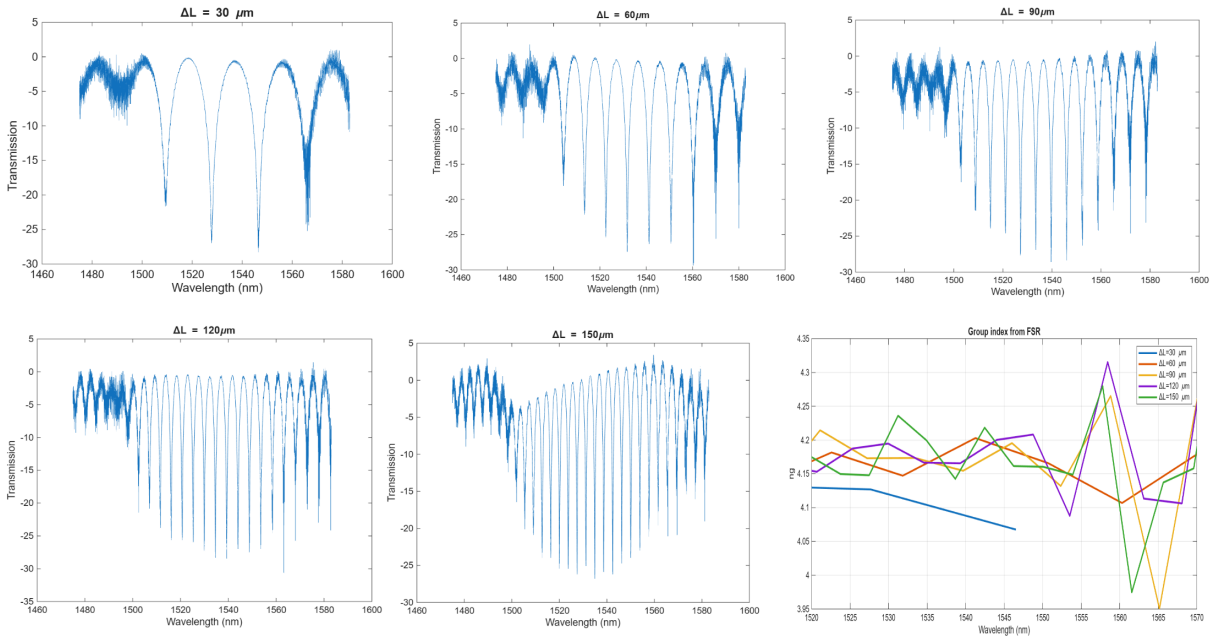

Fig. 5. Output signal measured from the MZI devices. The last figure shows the group index calculated from the FSR values from each measurement as represented by the legend.

150 μm.

5. Conclusion

We were able to successfully fabricate functional MZIs. The experimentally measured FSRs of each MZI device is in close agreement with the initial design. Furthermore, the group index calculated from the measurements lies close to the values predicted using the corner analysis.

6. References

[1]. Marchisio, A., Da Ros, F., Curri, V. et al. Comprehensive model of MZI-based circuits for photonic computing applications. Commun Phys 8(277), 2025.

[2]. Yadav, A., Kumar, A., Prakash, A., Design and analysis of optical switches using electro-optic effect based Mach-Zehnder interferometer structures. materialstoday 56(1), 2022.

[3]. Ultrafast Silicon MZI Optical Switch With Periodic Electrodes and Integrated Heat Sink. Journal of Lightwave Technology 39(15), 2021

[4]. Study on the limit of detection in MZI-based biosensor systems. Scientific Reports 9(5767), 2019.

[5]. L. Chrostowski and M. Hochberg, “Silicon Photonics Design: From Devices to Systems”, Cambridge University Press, 2015. [6]. R. J. Bojko, J. Li, L. He, T. Baehr-Jones, M. Hochberg, and Y. Aida, ”Electron beam lithography writing strategies for low loss, high confinement silicon optical waveguides,” J. Vacuum Sci. Technol. B 29, 06F309 (2011)

[7]. Lukas Chrostowski, Michael Hochberg, chapter 12 in ”Silicon Photonics Design: From Devices to Systems”, Cambridge University Press, 2015

[8]. http://siepic.ubc.ca/probestation, using Python code developed by Michael Caverley.

[9]. Yun Wang, Xu Wang, Jonas Flueckiger, Han Yun, Wei Shi, Richard Bojko, Nicolas A. F. Jaeger, Lukas Chrostowski, "Focusing sub-wavelength grating couplers with low back reflections for rapid prototyping of silicon photonic circuits", Optics Express Vol. 22, Issue 17, pp. 20652-20662 (2014) doi: 10.1364/OE.22.020652

[10]. www.plcconnections.com, PLC Connections, Columbus OH, USA.

[11]. http://mapleleafphotonics.com, Maple Leaf Photonics, Seattle WA, USA.

6.1. Acknowledgments:

I acknowledge the edX UBCx Phot1x Silicon Photonics Design, Fabrication and Data Analysis course, which is supported by the Natural Sciences and Engineering Research Council of Canada (NSERC) Silicon Electronic-Photonic Integrated Circuits (SiEPIC) Program. The devices were fabricated by Richard Bojko at the University of Washington Washington Nanofabrication Facility, part of the National Science Foundation's National Nanotechnology Infrastructure Network (NNIN), and Cameron Horvath at Applied Nanotools, Inc. Omid Esmaeeli performed the measurements at The University of British Columbia. We acknowledge Lumerical Solutions, Inc., Mathworks, Mentor Graphics, Python, and KLayout for the design software.